CaMK4-dependent activation of AKT/mTOR and CREM-α underlies autoimmunity-associated Th17 imbalance

Tomohiro Koga,[1] Christian M. Hedrich,[1,2] Masayuki Mizui,[1] Nobuya Yoshida,[1] Kotaro Otomo,[1] Linda A. Lieberman,[1] Thomas Rauen,[1,3] José C. Crispín,[1] and George C. Tsokos[1]

[1]Division of Rheumatology, Department of Medicine, Beth Israel Deaconess Medical Center, Harvard Medical School, Boston, Massachusetts, USA. [2]Pediatric Rheumatology and Immunology, University Children's Hospital Dresden, Dresden, Germany. [3]Department of Nephrology and Clinical Immunology, RWTH University of Aachen, Aachen, Germany.

Tissue inflammation in several autoimmune diseases, including SLE and MS, has been linked to an imbalance of IL-17–producing Th (Th17) cells and Tregs; however, the factors that promote Th17-driven autoimmunity are unclear. Here, we present evidence that the calcium/calmodulin-dependent protein kinase IV (CaMK4) is increased and required during Th17 cell differentiation. Isolation of naive T cells from a murine model of lupus revealed increased levels of CaMK4 following stimulation with Th17-inducing cytokines but not following Treg, Th1, or Th2 induction. Furthermore, naive T cells from mice lacking CaMK4 did not produce IL-17. Genetic or pharmacologic inhibition of CaMK4 decreased the frequency of IL-17–producing T cells and ameliorated EAE and lupus-like disease in murine models. Inhibition of CaMK4 reduced *Il17* transcription through decreased activation of the cAMP response element modulator α (CREM-α) and reduced activation of the AKT/mTOR pathway, which is known to enhance Th17 differentiation. Importantly, silencing CaMK4 in T cells from patients with SLE and healthy individuals inhibited Th17 differentiation through reduction of *IL17A* and *IL17F* mRNA. Collectively, our results suggest that CaMK4 inhibition has potential as a therapeutic strategy for Th17-driven autoimmune diseases.

Introduction

IL-17–producing CD4+ Th 17 (Th17) cells are defined by specific developmental and functional features that are distinct from those of "classical" Th1 and Th2 cells (1, 2). Th17 cells produce primarily two members of the IL-17 family, IL-17A and IL-17F, which promote local chemokine production to recruit monocytes and neutrophils to sites of inflammation (3). By amplifying inflammation, Th17 cells are thought to play a key role in the development and pathogenesis of various autoimmune diseases, including MS, rheumatoid arthritis, psoriasis, and SLE (4–8). Tregs, defined by constitutive expression of the high-affinity IL-2 receptor CD25 and the transcription factor FOXP3, are of major importance in protecting against immune-mediated pathology and the unrestricted expansion of effector T cell populations (9). Accordingly, both altered generation of Tregs and insufficient suppression of inflammation in autoimmune diseases are considered to be crucial for the initiation and perpetuation of disease. Taken together, the balance between Th17 cells and Tregs is of major importance in autoimmunity (10).

MS is a demyelinating disease of the human central nervous system mediated by autoreactive CD4+ T cells with specificity for myelin antigens (11). The Th1 and Th17 lineage of effectors has been implicated in the inflammatory response against central nervous system autoantigens (12). This widely accepted theory about the pathology of MS was based on data from experiments with EAE, the animal model of MS. SLE is an autoimmune disorder characterized by chronic inflammation that can affect virtually any organ and the presence of autoantibodies directed mostly against nuclear antigens (7). Patients with SLE or lupus-prone mice exhibit an imbalance between Th17 cells and Tregs (13), which can partly be explained by deficient IL-2 production, as IL-2 is necessary for the maintenance of Tregs and inhibition of Th17 differentiation (14–17). Low numbers of Tregs, along with high numbers of Th17 cells, could contribute to organ damage in SLE triggered by immune complexes, autoantibodies, inflammatory cytokines, and activated T cells.

Calcium/calmodulin-dependent protein kinase IV (CaMK4) is a multifunctional serine/threonine kinase that regulates several cellular processes, including gene expression (18). We have reported previously that CaMK4 is abnormally increased in T cells from patients with SLE (19) and lupus-prone mice (20). Furthermore, we have demonstrated that CaMK4 can directly inhibit IL-2 production by activating the repressor activity of cAMP response element modulator α (CREM-α) (19, 20). In line with these observations, genetic or pharmacologic inhibition of CaMK4 in MRL/*lpr* mice resulted in a significant decrease of autoantibody production, mesangial cell proliferation, improved Treg function, and improvement of lupus-related pathology and the survival rates (20–22). However, the molecular mechanisms whereby CaMK4 controls the generation of Th17 cells and suppression of Treg function in vitro and in vivo remain unclear.

Here, we demonstrate that inhibition of CaMK4 reduces the severity of EAE in C57BL/6J (B6) mice and that pharmacologic inhibition of CaMK4 in MRL/*lpr* mice corrects the imbalance between Tregs and Th17 cells in vitro and in vivo. We document that the CaMK4 effects are mediated through the AKT/mTOR pathway and through epigenetic remodeling mediated by the CaMK4-CREM-α axis. In line with these observations, silencing of CaMK4 in SLE T cells decreased the expression of IL-17–related cytokines upon stimulation in the presence of TGF-β and IL-6.

Conflict of interest: The authors have declared that no conflict of interest exists.

Citation for this article: *J Clin Invest.* 2014;124(5):2234–2245. doi:10.1172/JCI73411.

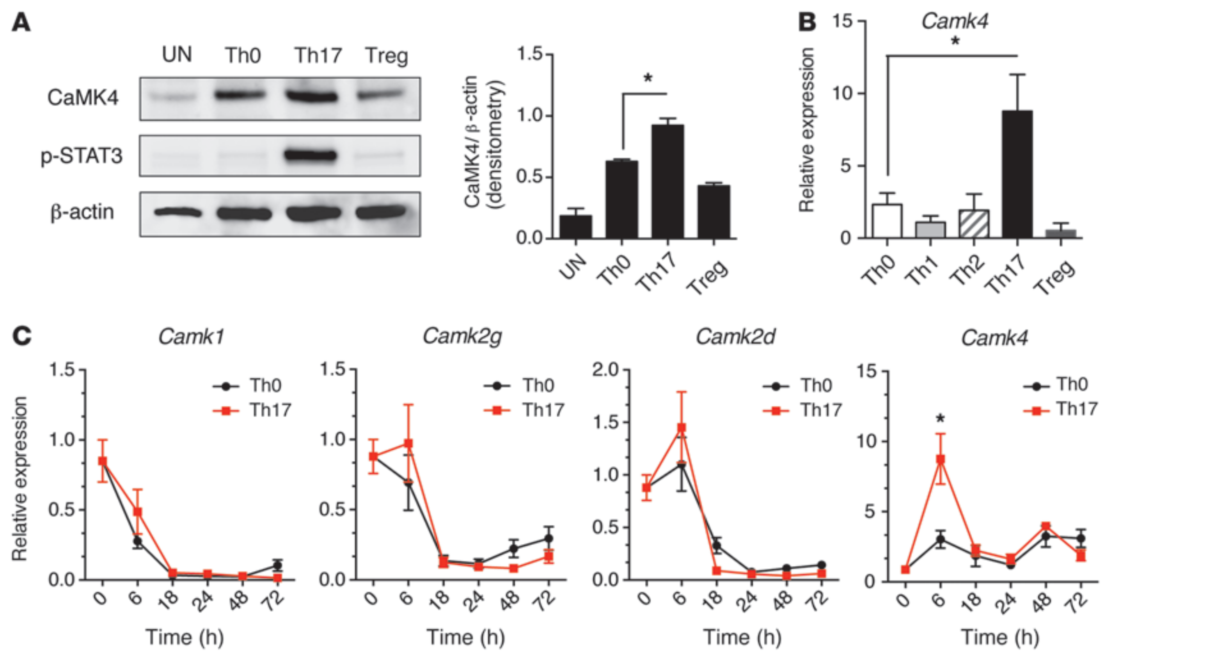

Figure 1
CaMK4 is induced during Th17 differentiation. (**A**) Western blot analysis of CaMK4 and phospho-STAT3 in unstimulated (UN) cells from MRL/*lpr* mice and cells stimulated under Th0, Th17, and Treg conditions. Cumulative data of densitometry is also shown (*$P < 0.05$; mean ± SEM; $n = 3$). (**B**) Real-time PCR analysis of *Camk4* mRNA in naive $CD4^+$ T cells from MRL/*lpr* mice stimulated 6 hours in Th0-, Th1-, Th2-, Th17-, or Treg-polarizing conditions. Results were normalized to *Gapdh* (*$P < 0.05$; mean ± SEM; $n = 4$). (**C**) Expression of *Camk1*, *Camk2d*, *Camk2g*, and *Camk4* mRNA in naive $CD4^+$ T cells at different time points during Th0 or Th17 differentiation (*$P < 0.05$; mean ± SEM; $n = 4$–5). Data are representative of 3 independent experiments.

Our findings suggest that both the CaMK4-AKT-mTOR and the CaMK4-CREM-α axes are involved in the imbalance between Th17 cells and Tregs in autoimmune disease, thus revealing possible therapeutic targets for the treatment of Th17 cell–mediated inflammatory diseases.

Results

CaMK4 expression is induced preferentially during Th17 differentiation. CaMK4 expression and activity is increased in T cells from patients with SLE (19, 20) and MRL/*lpr* lupus-prone mice (refs. 19, 20, and Supplemental Figure 1; supplemental material available online with this article; doi:10.1172/JCI73411DS1). To gain a better understanding of the role that CaMK4 plays in T cell function, we isolated naive CD4 T cells from MRL/*lpr* mice and stimulated them in the absence (Th0) or presence of polarizing cytokines to generate either Th17 cells (TGF-β + IL-6) or Tregs (TGF-β + IL-2) (10, 23). As shown in Figure 1A, T cell stimulation caused an increase in the levels of CaMK4 at the protein level. This was particularly marked in T cells stimulated under Th17-polarizing conditions (Figure 1A, lane 3) and dampened by Treg-inducing cytokines (Figure 1A, lane 4). To determine whether this effect was specific for the Th17-polarizing program, we differentiated naive CD4 T cells into Th1, Th2, and Th17 cells and Tregs and quantified *Camk4* expression by real-time PCR. As shown in Figure 1B, *Camk4* induction was significantly stronger in Th17 cells than in the other CD4 functional subsets. In order to clarify how the Th17-polarizing cytokines enhance the expression of CaMK4, we measured CaMK4 expression upon IL-1β, TGF-β, and/or IL-6 stimulation. Importantly, *Camk4* mRNA was induced modestly by IL-6, TGF-β, or IL-1β alone but was induced significantly more by the combination of IL-6 and TGF-β and that of IL-6, TGF-β, and IL-1β. Induced *Camk4* was inhibited by STAT3 or SMAD3 inhibitors, indicating that both signals are necessary for *Camk4* induction under Th17 conditions (Supplemental Figure 2). Although IL-1β is crucial for the induction of Th17-producing cells (24), IL-1β did not have an additional effect when combined with Th17-promoting cytokines (IL-6 and TGF-β) in increasing CaMK4 (Supplemental Figure 2). CaMK4 is a member of a family of serine/threonine kinases that includes CaMK1, CaMK2γ, CaMK2δ, and CaMK4 (25). To determine the specificity of Th17-induced expression of CaMK4, we stimulated naive CD4 T cells under neutral (Th0) or Th17-inducing conditions and analyzed the expression of members of the CaMK4 family by real-time PCR at different time points (Figure 1C). Expression of *Camk1*, *Camk2g*, and *Camk2d* did not differ when cells were stimulated under Th0- and Th17-polarizing conditions. In sharp contrast, *Camk4* expression was significantly higher early during Th17 differentiation. These results indicate that CaMK4 is preferentially induced during Th17 polarization. This phenomenon is particularly relevant, since patients with SLE and MRL/*lpr* mice have an increased abundance of IL-17–producing $CD4^+$ and $CD4^-CD8^-$ T cells (5, 26) and IL-17 has been associated with organ damage in lupus (5, 23).

CaMK4 is necessary for in vitro Th17 differentiation. To determine whether CaMK4 plays a role in Th17 cell differentiation, we isolated naive CD4 T cells from WT or *Camk4*$^{-/-}$ OT-II mice and stimulated them under Th17-polarizing conditions. As shown in Figure 2A, absence of *Camk4* caused a significant decrease in the percentage of IL-17–producing T cells ($P = 0.0046$). To expand these results, we transfected cells from *Camk4*-sufficient (*Camk4*$^{+/+}$)

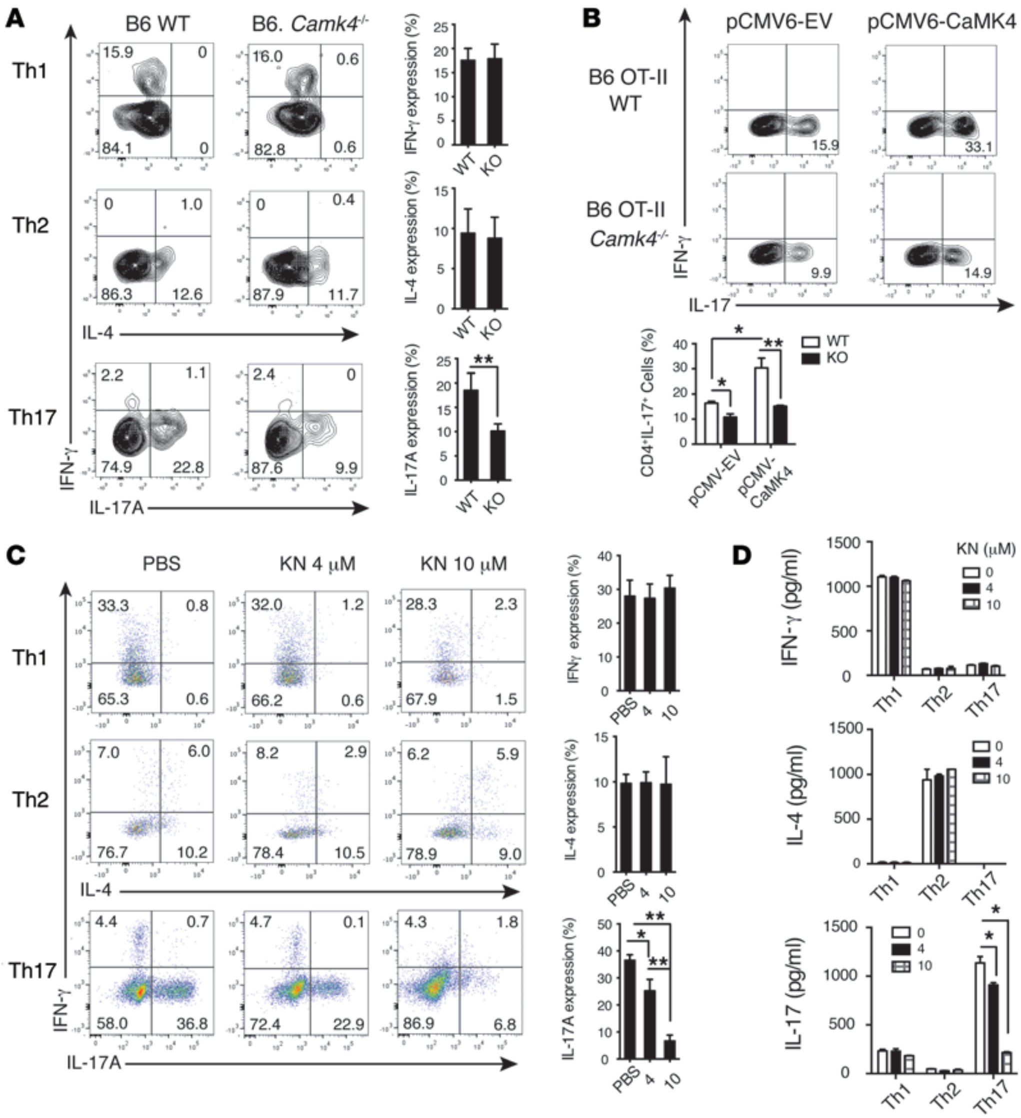

Figure 2

CaMK4 controls the development of Th17 cells. (**A**) Naive T cells differentiated for 72 hours in Th1, Th2, or Th17 conditions from spleens of B6 or B6.*Camk4*$^{-/-}$ mice were gated on TCRβ$^+$CD4$^+$ and stained for intracellular expression of IFN-γ, IL-4, and IL-17A. A profile representative of 4 mice per group is shown (**$P < 0.01$; mean ± SEM). (**B**) OT-II (WT or *Camk4*$^{-/-}$) cells were transfected with either empty vector or pCMV-CaMK4. 4 hours after transfection cells were stimulated under Th17 conditions. After 48 hours, IL-17–producing TCRβ$^+$CD4$^+$ T cells were measured by intracellular cytokine staining. A profile representative of 4 mice per group is shown (*$P < 0.05$, **$P < 0.01$; mean ± SEM). (**C**) Naive T cells differentiated for 72 hours in Th1, Th2, or Th17 conditions in the presence of different concentrations of KN-93 from spleens of MRL/*lpr* mice (16 weeks old) were gated on TCRβ$^+$CD4$^+$ and stained for intracellular expression of IFN-γ, IL-4, and IL-17A. A profile representative of 3 independent experiments with 3 to 5 mice per group is shown (*$P < 0.05$, **$P < 0.01$; mean ± SEM). (**D**) ELISA of IFN-γ, IL-4, and IL-17 in supernatants of naive T cells from MRL/*lpr* mice differentiated for 72 hours in Th1, Th2, or Th17 conditions in the presence of different concentrations of KN-93 (μM). (*$P < 0.05$; mean ± SEM; n = 3–5). Data are representative of 3 independent experiments with 3 to 5 mice.

or -deficient (*Camk4*$^{-/-}$) OT-II mice with either an empty vector or a *Camk4*-encoding plasmid. This allowed us to evaluate WT cells with normal and augmented abundance of CaMK4 side by side *Camk4*-deficient cells before and after CaMK4 reconstitution (Supplemental Figure 3). Cells were then stimulated in Th17-polarizing conditions, and the frequency of IL-17–producing cells was quantified by flow cytometry (Figure 2B). As expected, absence of *Camk4* resulted in fewer IL-17$^+$ T cells (P = 0.0321). However, reconstitution of *Camk4* restored the IL-17 production defect, and, importantly, *Camk4* overexpression led to increased numbers of IL-17–producing cells (P = 0.0378; Figure 2B). KN-93 is an inhibitor of CaMK4 (27) that ameliorates disease in lupus-prone mice (21). We stimulated naive CD4 T cells in Th1-, Th2-, and Th17-polarizing conditions in the presence of 2 concentrations of KN-93 (4 and 10 μM). As shown in Figure 2C, KN-93 inhibited Th17 differentiation and IL-17 production in a dose-dependent manner (PBS vs. 4 μM, P = 0.0142; PBS vs. 10 μM, $P < 0.0001$). Consistent with these observations, mRNA levels of Th17 transcription factors and Th17 cell–associated cytokines were also decreased in the presence of KN-93 (Supplemental Figure 4). Conversely, its effects on the differentiation of Th1 and Th2 cells were negligible (Figure 2, C and D). Taken together, these data indicate that CaMK4 is a necessary element in Th17 differentiation and IL-17 production that can be modulated by a pharmacologic inhibitor of CaMK4.

Camk4 deficiency ameliorates EAE. To evaluate the relevance of CaMK4 in an IL-17–dependent inflammatory condition, we induced EAE (28) in *Camk4*-sufficient (WT) and -deficient mice by immunizing with myelin oligodendrocyte glycoprotein (MOG_{35-55}) (29). WT mice developed signs of EAE on day 11 and reached the peak of the disease on day 15 after immunization. In contrast, in *Camk4*$^{-/-}$ mice, disease onset was delayed and was significantly less severe when quantified as a clinical score (P = 0.0318; Figure 3A) or percentage of weight loss (P = 0.0464; Figure 3B).

To determine whether CaMK4 inhibition ameliorated EAE by decreasing the differentiation of Th17 cells, we immunized WT and *Camk4*$^{-/-}$ mice with MOG_{35-55} and quantified the frequency of IL-17– and IFN-γ–producing cells 8 days later. As predicted by our in vitro results, CaMK4 deficiency reduced significantly the number of IL-17⁺ CD4 T cells in the spleens and draining inguinal lymph nodes of immunized mice, without affecting the production of IFN-γ (Figure 3C). Independent histological analysis of spinal cords demonstrated significantly decreased inflammation and demyelination in *Camk4*$^{-/-}$ mice (Figure 4).

CaMK4 inhibition limits the production of IL-17 in MRL/lpr mice. CaMK4 expression and activity is increased in T cells from patients with SLE and lupus-prone mice (19, 20), and IL-17 has been suggested to play a role in target organ damage in lupus, including glomerulonephritis (30, 31). Therefore, we treated MRL/*lpr* mice with KN-93 for 10 weeks and examined IL-17A expression in spleens and lymph nodes during the peak of the disease (~16 weeks of age). KN-93 treatment led to a significant decrease in IL-17–producing CD4$^+$ and CD4$^-$CD8$^-$ (double-negative [DN]) T cells in spleens and in lymph nodes from mice treated with KN-93 (Figure 5, A and B). In line with these observations, mRNA levels of *Rorc*, the master regulator of Th17 cells (32), were also reduced by pharmacologic inhibition of CaMK4 (Figure 5C). The inhibitory effects of KN-93 were specific for IL-17, since it did not modify the frequency of IFN-γ–producing cells or the expression of the Th1- and Th2-associated transcription factors *Tbx21* and *Gata3*, respectively (Figure 5, B and C). KN-93 treatment decreased significantly the mortality of MRL/*lpr* mice (Figure 5D) as well as serum titers of anti–double-stranded DNA antibodies at 12 and 16 weeks of age and proteinuria at 16 weeks of age (Supplemental Figure 5), confirming the relevance of IL-17 inhibition in this lupus model.

CaMK4 promotes transcription of Il17 through CREM-α. Methylation of CpG-DNA is associated with decreased transcription of neighboring genes (33). To investigate the mechanisms that regulate IL-17A expression during Th17 differentiation, we examined the CpG-DNA methylation of regulatory conserved noncoding sequences (CNSs) of the *Il17* gene in CD4$^+$ T cells from MRL/*lpr* and MRL/*lpr.Camk4*$^{-/-}$ mice (Supplemental Figure 6). After 24 hours of activation with anti-CD3 and anti-CD28 antibodies, CD4$^+$ T cells from MRL/*lpr* mice exhibited low degrees of CpG-DNA methylation in all investigated regions of the *Il17* locus (Figure 6A). In contrast, cells from MRL/*lpr* mice deficient in *Camk4* had significantly higher levels of methylation (CNS1, $P = 0.0382$; CNS2, $P = 0.0353$). These results suggested that CaMK4 regulates IL-17 production by controlling its transcription. Since the phosphorylation and DNA-binding activity of the transcription factor CREM-α is regulated by CaMK4 (19, 20) and CREM-α has been shown to modulate *IL17* transcription in T cells from patients with SLE (34, 35), we hypothesized that CaMK4 might control IL-17 expression through CREM-α. To evaluate this possibility, we analyzed the binding of CREM-α to consensus cAMP response element (CRE) sites within the *Il17* promoters of CD4$^+$ T cells from MRL/*lpr* and MRL/*lpr.Camk4*$^{-/-}$ mice by ChIP. As shown in Figure 6B, we detected reduced recruitment of CREM-α to CREs in the *Il17* promoters of *Camk4*-deficient MRL/*lpr* mice. These results indicate that, through promoting the DNA-binding activity of CREM-α, CaMK4 facilitates *Il17* transcription.

To investigate whether CaMK4 regulates IL-17 expression at the transcriptional level, we cloned the *IL17* promoter into a luciferase reporter system (36). This promoter region includes CRE and ROR element binding sites (35). As shown in Figure 6C, the cloned promoter region possessed transcriptional activity that was completely abrogated in cells treated with KN-93 or *Camk4*-specific siRNA, indicating that CaMK4 promotes the transcriptional activity of IL-17. As expected, the activity of the promoter was partially abrogated when the CRE site (–111/–104) was mutated and was completely lost when both the CRE and the ROR element binding sites (–140/–135) were mutated. CaMK4 inhibition by KN-93 or siRNA was still able to decrease the transcriptional activity of the promoter in the absence of the CRE site, suggesting that CaMK4 promotes *Il17* transcription both through the CRE and the ROR element binding sites.

CaMK4 promotes AKT/mTOR signaling. The activation of mTORC1 enhances Th17 differentiation (37) and disruption of mTORC1 caused by deletion of *Rheb* or *Raptor* impairs Th17 differentiation (38, 39). CaMKs, including CamK4, have been reported to modulate the AKT signaling pathway (40, 41). Therefore, CaMK4 might promote IL-17 production by facilitating AKT/mTOR signaling. To test this hypothesis, we first established the physical association between AKT and CaMK4 by performing coimmunoprecipitation experiments (Figure 7A). Next, we analyzed the effect of KN-93 on the AKT/mTOR pathway activity induced by T cell stimulation. Western blots of cell lysates revealed that KN-93 significantly inhibited AKT phosphorylation in a dose-dependent manner (Figure 7B). KN-93 also inhibited the phosphorylation of p70S6, a substrate of mTOR (Figure 7C). These results were confirmed using T cells from *Camk4*$^{-/-}$ mice cultured in vitro under Th0- or Th17-polarizing conditions in the presence of OVA peptide (5 μM). As shown in Figure 7, D and E, phosphorylation of AKT and p70S6 was clearly decreased in the absence of *Camk4*. To further establish these findings, we incubated Jurkat T cells with KN-93 and quantified AKT and S6K phosphorylation by flow cytometry. KN-93 decreased AKT and S6K phosphorylation in Jurkat T cells (Supplemental Figure 7A). In concordance, overexpression of CaMK4 in Jurkat T cells induced increased AKT and S6K phosphorylation (Supplemental Figure 7B). Taken together, these results demonstrate that CaMK4 facilitates AKT/mTOR signaling. To determine whether CaMK4 promotes IL-17 production by facilitating AKT/mTOR signaling, we treated *Camk4*-overexpressing T cells with the mTORC1 inhibitor rapamycin (100 nM). mTORC1 blockade abrogated IL-17 production induced by CaMK4 overexpression (Supplemental Figure 8).

Silencing of CaMK4 suppresses Th17 cells in human T cells. To determine the relevance of our findings in human T cells, we analyzed the effect of CaMK4 inhibition in T cells from healthy donors or patients with SLE. We first asked whether KN-93 can inhibit Th17 differentiation in controls. As expected, KN-93–treated T cells displayed a substantial reduction of IL-17–producing cells in a dose-dependent manner (Figure 8A). To determine the effects of CaMK4 inhibition on IL-17 expression in T cells from patients with SLE, we stimulated cells transfected with *CAMK4*-specific or control siRNA with anti-CD3, anti-CD28, IL-6, and TGF-β. As shown in Figure 8B, CaMK4 inhibition decreased significantly *IL17A* and *IL17F* mRNA levels in cells from healthy donors and patients with SLE. Taken together, our results indicate that CaMK4 positively regulates IL-17 production in T cells from healthy donors and patients with SLE.

Discussion

Recent data support the role of the effector cytokine IL-17A and Th17 cells in the pathogenesis of SLE and other autoimmune disorders, including MS. It has been noted that patients with SLE, including those with new-onset disease, display increased serum or plasma levels of IL-17A, expansion of IL-17–produc-

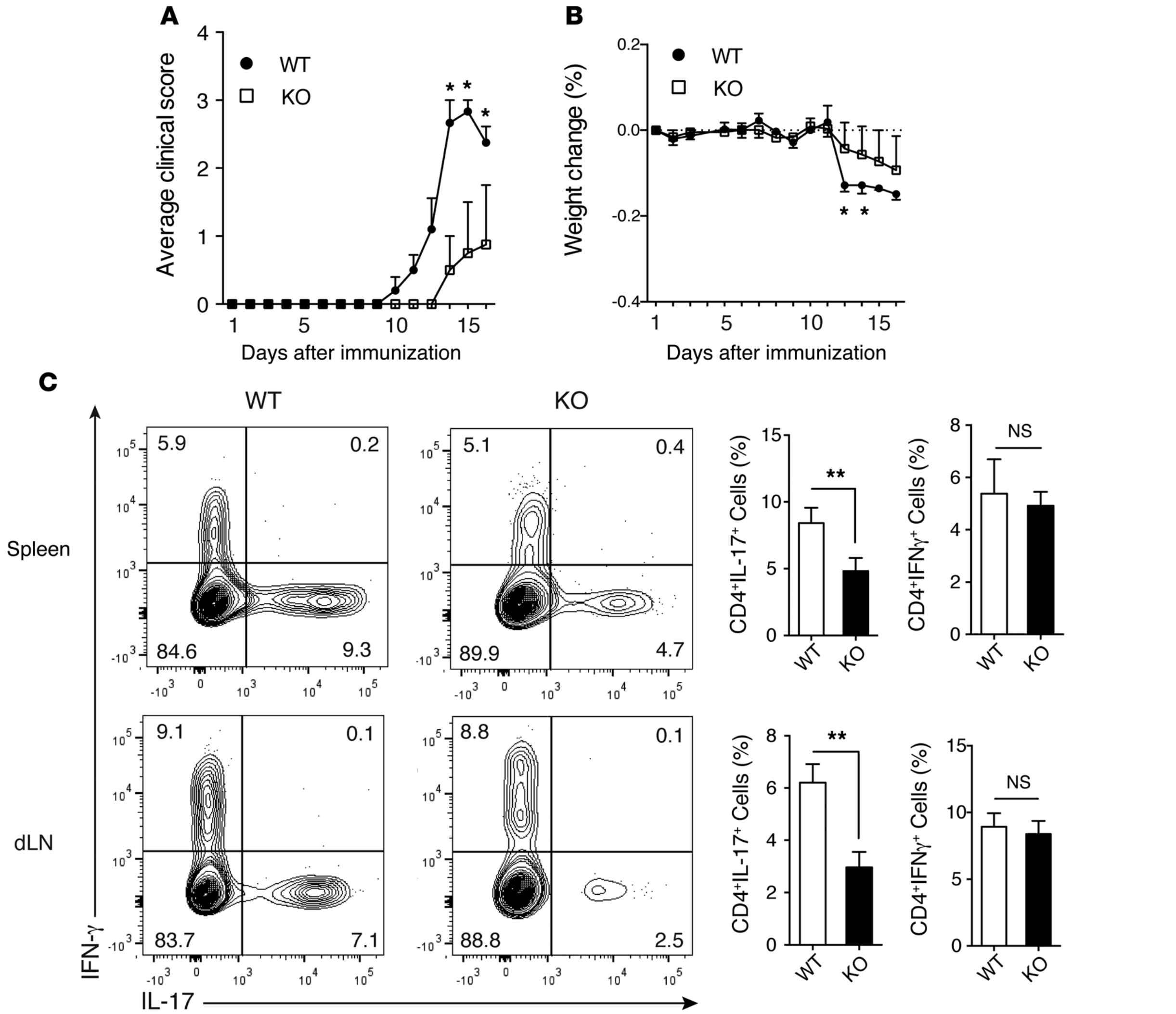

Figure 3

Camk4$^{-/-}$ mice are resistant to EAE. EAE was induced in WT and *Camk4*$^{-/-}$ mice by immunization with $MOG_{35–55}$ emulsified in CFA. (**A**) The clinical score of EAE and (**B**) body weight in these mice were monitored (*P < 0.05; mean ± SEM; cumulative results of 3 independent experiments with 3 to 5 mice per group). (**C**) Flow cytometry of intracellular IL-17 and IFN-γ at day 8 in $CD4^+$ T cells obtained from mononuclear cells isolated from the draining inguinal lymph nodes (dLNs) and spleens of WT and *Camk4*$^{-/-}$ mice immunized with $MOG_{35–55}$ emulsified in CFA to induce EAE and then activated in vitro with PMA and ionomycin (**P < 0.01; mean ± SEM; n = 3–4). Data are representative of 2 independent experiments with 3 to 4 mice per group.

ing T cells in the peripheral blood, and infiltration of Th17 cells in target organs, including the kidneys (42, 43). Also, increased production of IL-17A in patients with SLE correlates with disease activity (44). Further, IL-17 has been implicated in the expression of organ pathology in lupus-prone mice (30, 44–46). Prior reports from our group have indicated the presence of IL-17–producing DN T cells in the kidneys of patients with SLE and those of the lupus-prone MRL/*lpr* and B6.*lpr* mice (26, 47). Tregs display suppressive activity against autoreactive lymphocytes, thus preventing or mitigating the onset of aberrant self-immune response (48). Most studies that examined the role of Tregs in SLE reported either reduced numbers or impaired function of circulating Tregs (49, 50). Accordingly, evidence suggests that aberrant T cell homeostasis and Th17/Treg imbalance represent an important key pathogenic player.

Here, we provide evidence that CaMK4 is important in the generation of Th17 cells and that elevated IL-17 cytokine production mediated by CaMK4 plays an important role in the fatal outcome in MRL/*lpr* mice and in EAE. Our work identifies CaMK4 as a critical molecule involved in the imbalance between Th17 and Tregs in autoimmunity.

Aberrant cytokine expression caused by an impaired transcriptional network is a hallmark of the pathogenesis of autoimmune diseases, including SLE and MS (51, 52). We reported recently that CaMK4 can activate the transcription factor CREM-α (19, 20), which mediates epigenetic remodeling of cytokine genes, including *IL17* during the priming of $CD4^+$ T cells from patients with SLE (35, 53). Consistent with this, MRL/*lpr.Camk4*$^{-/-}$ mice exhibited reduced CREM-α recruitment to the *Il17* promoter, which led to decreased IL-17, arguing that the CaMK4-CREM-α

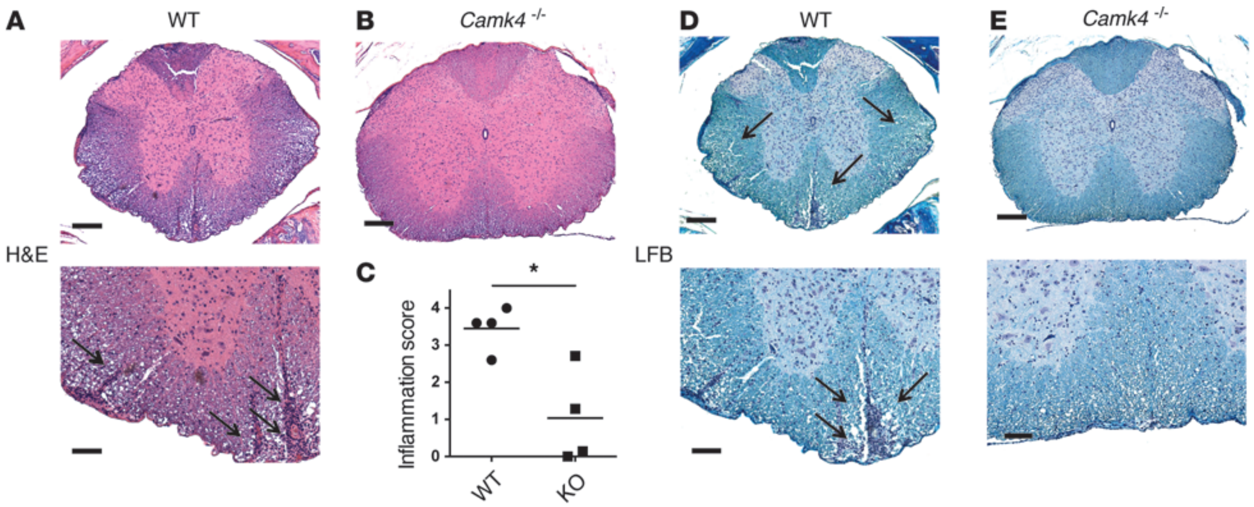

Figure 4
Camk4–/– mice display less inflammation and demyelination in EAE. Spinal cord sections from WT and *Camk4*–/– mice obtained at 14 days after immunization. Sections were stained with (**A** and **B**) H&E to assess inflammation and (**D** and **E**) luxol fast blue to assess myelin content. Arrows indicate inflammatory cellular infiltrates. Scale bars: 50 μm (top rows); 200 μm (bottom rows). Quantitative cumulative data (n = 4 mice per group) are shown in **C** (*P < 0.05).

axis is active in lupus-prone mice and may be central to disease expression. To determine whether epigenetic changes are strain specific, we examined the methylation status of the *Il17a* loci from B6 and B6 *Camk4* KO mice under Th17 conditions. We did not observe any significant differences in the methylation index in the B6 background (data not shown). Because we have already shown that CREM-α is expressed more in MRL/*lpr* mice (54) and T cells from patients with SLE (55), we speculate that CaMK4 deficiency can inhibit CREM-α function only in the MRL background.

In this study, we demonstrate that CaMK4 activity is the highest under Th17-polarizing conditions, and KN-93, a known CaMK4 inhibitor, can alter Th17 and Treg differentiation but not that of Th1 or Th2 in MRL/*lpr* mice. This specific involvement of CaMK4 in the differentiation of Th17 cells solely, without affecting the differentiation of Th1 and Th2 cells, was unexpected and urges the consideration of pharmacologic inhibition of CaMK4 in the treatment of Th17-dependent inflammatory diseases.

The PI3K/AKT/mTOR pathway is an intracellular signaling pathway that is important in several normal cellular functions that are also critical for tumorigenesis, including cellular proliferation, growth, survival, and mobility (56). It was reported recently that the PI3K-AKT-mTORC1-S6K axis positively regulates Th17 differentiation by promoting the nuclear translocation of RORγt (37, 39). Here, we showed that pharmacologic inhibition of CaMK4 by KN-93 or genetic deletion of *Camk4* in OT-II mice impairs the phosphorylation of S6K, indicating an importance of the CaMK4/AKT/mTOR pathway in the regulation of Th17 differentiation. Prior reports have suggested that mTOR inhibitor, rapamycin, improved the clinical course of lupus nephritis and prolong survival in NZBW/F1 mice (57) as well as MRL/*lpr* mice (58). Moreover, this drug reduced disease activity in patients with SLE who had been treated unsuccessfully with other immunosuppressive medications (59). However, it is important to note that distinct side effects have been recognized, including interstitial pneumonitis, anemia associated with chronic inflammation, and severe forms of glomerulonephritis (60, 61). These antiinflammatory responses of mTOR inhibition have been mainly observed in monocytes, macrophages, and peripheral myeloid dendritic cells (62). Although AKT/mTOR pathway–related proteins are expressed in most immune cells, CaMK4 is restricted to T cells, suggesting that inhibition of CaMK4 may represent a more specific therapeutic option in Th17-mediated diseases, with potentially reduced side effects.

In conclusion, we have provided evidence that CaMK4 plays a central role in reversing the balance between Th17 cells and Tregs in favor of Th17 cells and the development of organ damage in MRL/*lpr* mice as well as in mice provoked to develop EAE. CaMK4 promotes Th17 cell differentiation and reduces the activity of Tregs. As depicted in Figure 9, CaMK4 uses two distinct pathways, the AKT/mTOR pathway and one which increases the binding of CREM-α to the *Il17* genes, followed by epigenetic modulation of their activity (63). We have not addressed the relative contribution of each pathway in the differentiation of Th17 cells and whether one or the other is sufficient alone for the production of IL-17. What is important though is the fact that CaMK4 is upstream of both of them and that its inhibition will avert IL-17–instigated inflammation.

Methods

Mice. Female MRL/MpJ-*Tnfrsf6*^{lpr} (MRL/*lpr*), B6.129X1-*Camk4*^{tm1Tch}/*J*, B6, OT-II (C57BL/6-Tg(*TcraTcrb*)425Cbn/J), and MRL/*MPJ* mice were purchased from The Jackson Laboratory. MRL/*lpr*.*Camk4*–/– mice have been described previously (20). OT-II.*Camk4*–/– mice were made by crossing B6 mice with OT-II mice. MRL/*lpr* mice were administrated with KN-93, a CaMK4 inhibitor (Calbiochem), as previously reported (21). Animals were sacrificed at the end of their 6th or 16th week of life. Mice were maintained in an SPF animal facility (Beth Israel Deaconess Medical Center). Experiments were approved by the Institutional Animal Care and Use Committee of Beth Israel Deaconess Medical Center.

In vitro T cell differentiation. Spleens and lymph nodes were excised from mice, and single-cell suspensions were obtained by teasing the organs through a nylon mesh. Naive $CD4^+$ T cells from the spleens and lymph nodes were then purified by magnetic cell sorting ($CD4^+CD62L^+$ T Cell Isolation Kit II; Miltenyi Biotec) or by a FACS Aria II cell sorter (BD Biosciences); the purity of

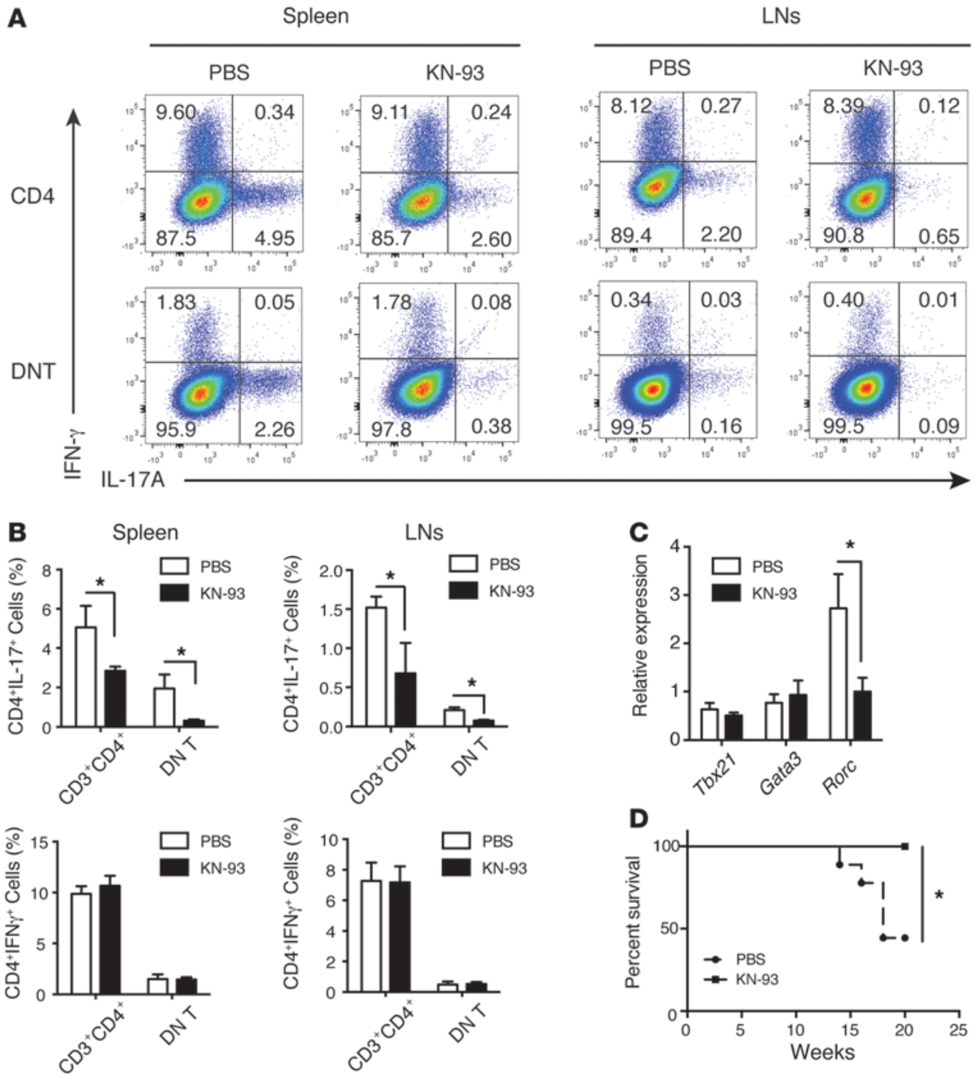

Figure 5

CaMK4 inhibition limits the production of IL-17 cytokines in MRL/*lpr* mice. (**A**) Cells from spleens and lymph nodes of PBS-treated and KN-93–treated MRL/*lpr* mice (16 weeks old) were gated on TCRβ$^+$CD4$^+$ and stained for intracellular expression of IL-17A and IFN-γ. Data are representative of 4 independent experiments with 4 to 5 mice per group. (**B**) Percentage of IL-17A–producing and IFN-γ–producing T subsets in spleens (n = 4–6) and LNs (n = 4–6). DN T cells are CD3$^+$CD4$^-$CD8$^-$ (*P < 0.05; mean ± SEM). (**C**) Quantitative real-time PCR analysis of the expression of *Tbx21*, *Gata3*, and *Rorc* mRNA in memory CD4$^+$ T cells (*P < 0.05; mean ± SEM; n = 4). (**D**) Survival of MRL/*lpr* mice treated with PBS or KN-93 is depicted. Mice were observed until 20 weeks of age (*P < 0.05; n = 8–10 mice per group). Cumulative results of 3 independent experiments with 3 to 5 mice per group.

isolated T cell populations routinely exceeded 95%. Naive T cells were stimulated with plate-bound goat anti-hamster antibodies, soluble anti-CD3 (0.25 μg/ml, clone 145-2C11; Biolegend) and anti-CD28 (0.5 μg/ml, clone 37.51; Biolegend), in the presence of IL-12 (20 ng/ml; R&D Systems) and anti–IL-4 (10 μg/ml; C17.8; Biolegend) for the generation of Th1 cells; IL-4 (100 ng/ml; R&D Systems), anti–IL-12 (10 μg/ml; Biolegend), and anti–IFN-γ (10 μg/ml; XMG1.2; Biolegend) for the generation of Th2 cells; IL-6 (100 ng/ml; R&D Systems), TGF-β1 (3 ng/ml; R&D Systems), anti–IL-4 (10 μg/ml; C17.8; Biolegend), and anti–IFN-γ (10 μg/ml; XMG1.2; Biolegend) for the generation of Th17 cells; or IL-2 (20 ng/ml; R&D Systems), TGF-β1 (3 ng/ml; R&D Systems), anti–IL-4 (10 μg/ml; C17.8; Biolegend), and anti–IFN-γ (10 μg/ml; XMG1.2; Biolegend) for the generation of Tregs. Assays with splenocytes from OT-II mice were done using the $OVA_{323–339}$ peptide (5 μM; Bio-Synthesis Inc.). For signal transduction studies, STAT3 inhibitor (10 μM; Calbiochem), SMAD3 inhibitor (10 μM; Calbiochem), and mTOR inhibitor rapamycin (100 nM; Calbiochem) were added to cultures.

EAE disease models. Mice were immunized with $MOG_{35–55}$ peptide emulsified in CFA (Sigma-Aldrich) containing 4 mg/ml *Mycobacterium tuberculosis* extract H37Ra (Difco) in 100 μl per mouse s.c. distributed between the 2 hind flanks and above the sternum on day 0. On days 0 and 2, 50 μg pertussis toxin (List Biological Laboratories) was given i.v. Subsequently, these mice were treated with KN-93 or PBS twice a week. Mice were monitored daily and clinical scores were given as follows: 1, limp tail; 2, hind-limb paresis; 3, hind-limb paralysis; 4, tetraplegia; 5, moribund.

Histological staining and analysis. Spinal cords (10% formalin fixed) were stained with H&E for detection of inflammatory infiltrates and luxol fast blue for myelin detection. Histological sections were scored by an investigator blinded to experimental group as follows: 0, no infiltration (<50 cells); 1, mild infiltration of nerve or nerve sheath (50–100 cells); 2, moderate infiltration (100–150 cells); 3, severe infiltration (150–200 cells); 4, massive infiltration (>200 cells).

Intracellular cytokine staining. For intracellular cytokine staining, cells were isolated as described above and were stimulated for 4 hours in culture medium containing PMA (50 ng/ml; Sigma-Aldrich), ionomycin (1 mg/ml; Sigma-Aldrich), and monensin (GolgiStop; 1 ml/ml; BD Biosciences). After staining of surface markers CD3e (17A2, eBioscience), CD4 (GK1.5, BioLegend), CD8a (53-6.7, eBioscience), or TCRβ (H57-597, BioLegend) for 30 minutes at 4°C, cells were fixed and made permeable with Cytofix/Cytoperm and Perm/Wash buffer according to the manufacturer's instructions (BD Biosciences). All antibodies to cytokines (anti–IFN-γ XMG1.2, anti–IL-4 11B11, and anti–IL-17A JC11-18H10.1) were from BioLegend. For the detection of phosphorylated signaling proteins, lymphocytes were fixed with 1.5% paraformaldehyde, followed by permeabilization with methanol and staining with antibodies to S6 phosphorylated at Ser 235 and Ser 236 (D57.2.2E; Cell Signaling Technology) and AKT phosphorylated at Ser 473 (D9E; Cell Signaling Technology).

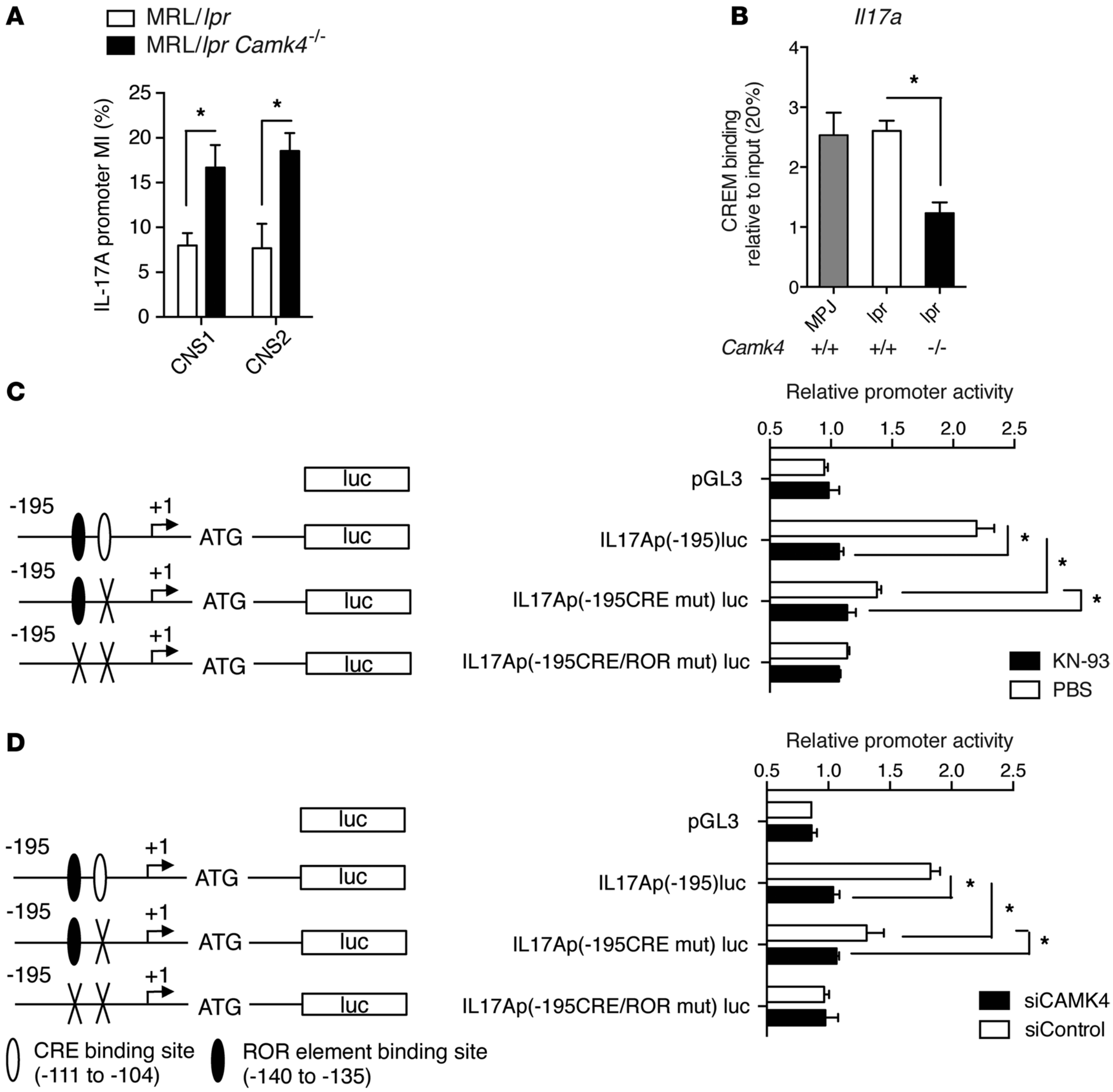

Figure 6

CaMK4 mediates CpG-DNA methylation of the *Il17a* gene through CREM-α. (**A**) CD4+ T cells from 14-week-old MRL/*lpr* and MRL/*lpr*.*Camk4*–/– mice were sorted for the assessment of CpG-DNA methylation of the *Il17a* promoter region using methylated CpG-DNA immunoprecipitation (*$P < 0.05$; mean ± SEM). Methylation index (MI), as assessed relative to methylated (100%) and unmethylated (0%) control DNA, is shown. Data are representative of 2 independent experiments with 4 mice per group. (**B**) CREM-α recruitment to the *Il17a* CRE-binding site in CD4+ T cells from MRL/MPJ, MRL/*lpr*, or MRL/*lpr*.*Camk4*–/– mice was detected by ChIP assay (*$P < 0.05$; mean ± SEM). Data are representative of 2 independent experiments with 4 mice per group. (**C** and **D**) Alignment of the CRE consensus sequence with the CRE site (–111/–104) and the ROR element binding site (–140/–135) of the proximal human IL-17A promoter is shown. Jurkat T cells were treated with (**C**) KN-93 (10 μM) or transfected with (**D**) either control siRNA or *CAMK4*-specific siRNA for luciferase assays using the IL-17A reporter plasmids. IL17Ap (-195mut)-luc indicates a reporter plasmid containing a site-directed mutation at the CRE site (–111/–104) and the ROR element binding site (–140/–135) (*$P < 0.05$; mean ± SEM; n =3–4). Cumulative results of 3 independent experiments.

RNA isolation and real-time RT-PCR. Total mRNA was isolated from spleen cells using the RNeasy Mini Kit (Qiagen) and then cDNA was synthesized using cDNA EcoDry Premix (Clontech) for PCR amplification. Expression was normalized to *Gapdh*. All primers and probes were from Applied Biosystems or OriGene: *Gata3* (Mm01337569_m1), *Tbx21* (Mm00450960_m1), *Rorc* (Mm00441144_g1), *Il17a* (Mm00439619_m1), *Il17f* (Mm00521423_m1), *Il21* (Mm00517640_m1), *Il22* (Mm00444241_m1), *Camk1* (Mm00519436_m1), *Camk2g* (MP201589), *Camk2d* (Mm00499266_m1), *Camk4* (Mm01135329_m1), *Gapdh* (Mm99999915_g1), *IL17A* (Hs00936345_m1), and *GAPDH* (4310884E). Gene expression was assessed by comparative C_T method.

ELISA. Splenic naive CD4+CD62+ T cells were stimulated as described above. After 72 hours, IFN-γ, IL-4, and IL17A were measured in supernatants by ELISA (BioLegend). Serum anti-dsDNA antibody concentration was detected by the mouse anti-dsDNA IgG ELISA kit (Alpha Diagnostic Intl. Inc.). Urinary albumin was quantified by ELISA (Bethyl Laboratories).

Western blotting. Splenocytes or T cells were lysed in RIPA buffer at 4°C for 30 minutes. After centrifugation (16,400 *g*; 30 minutes; 4°C), superna-

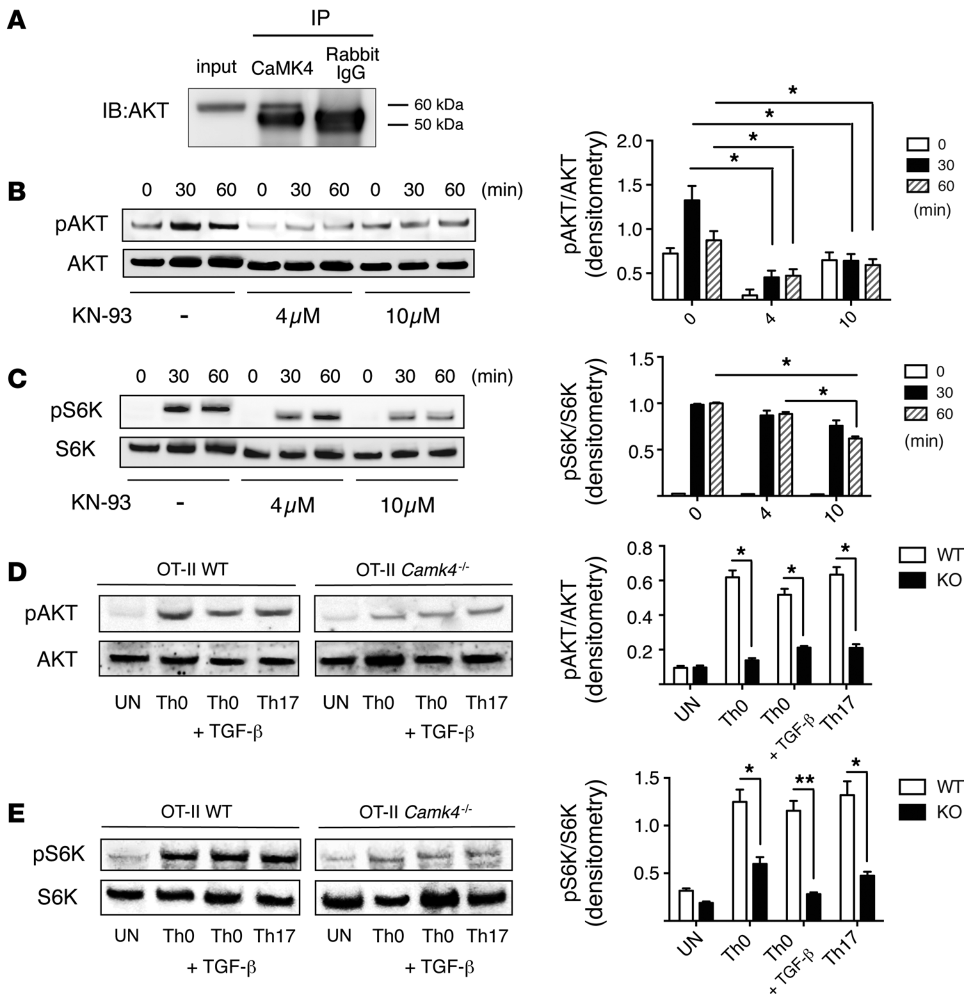

Figure 7

Inhibition of CaMK4 decreased Th17 differentiation through the blocking of the AKT/mTOR signaling pathway. (**A**) Immunoprecipitation and protein immunoblot analysis of AKT expression is shown. Jurkat T cells were stimulated with anti-CD3 and anti-CD28 antibodies for 20 minutes. Cell lysates were then prepared and immunoprecipitated with anti-CaMK4 or with a control rabbit antibody. The immunoprecipitates were then analyzed by immunoblotting using AKT antibody. The data are representative of 2 independent experiments. Western blotting analysis of (**B**) phospho-AKT and (**C**) phospho-S6K in $CD4^+$ T cells from MRL/*lpr* mice in unstimulated and Th17 conditions for the indicated times. Western blotting analysis of (**D**) phospho-AKT and (**E**) phospho-S6K in OT-II cells (WT or *Camk4*$^{-/-}$) in unstimulated, Th0 (with or without TGF-β), and Th17 conditions. The graphs in **B**–**E** show cumulative data of densitometry (*P < 0.05, **P < 0.01; mean ± SEM; n = 3–4). Data are representative of 3 independent experiments with 3 to 4 mice per group.

Gene expression plasmids transfections. T cells from OT-II WT mice or OT-II *Camk4*$^{-/-}$ mice were cultured for 16 to 18 hours in RPMI/Th0 conditions. 2 million stimulated cells were transiently transfected with 2 μg of mouse CaMK4 expression vectors (CaMK4 expression plasmid under the control of the CMV promoter) or empty vector (pCMV6) from OriGene Technologies. Transfections were performed using the Amaxa Mouse T Cell Nucleofector Kit with the X-001 program (Amaxa) according the manufacture's protocol. After 4 hours recovery at 37°C, cells were stimulated in Th17 conditions in RPMI media.

Methylated CpG-DNA immunoprecipitation. The methylated CpG-DNA immunoprecipitation assay was carried out according to the manufacturer's instructions (Zymo Research). Briefly, genomic DNA from T cells obtained from MRL/*lpr* mice or MRL/*lpr*.*Camk4*$^{-/-}$ mice was purified using the AllPrep RNA/DNA/Protein Mini Kit (Qiagen), sheared to fragments of approximately 200 bp using DNA Shearase (Zymo Research). Subsequently, 100 ng sheared genomic DNA was used for methylated CpG-DNA immunoprecipitation. Methylated DNA was recovered and subjected to PCR analysis. Real-time PCR primer sequences are given in Supplemental Table 1.

ChIP assays. Polyclonal anti–CREM-α antibody detecting mouse CREM-α has been described before (19). Nonspecific normal rabbit IgG was obtained from Invitrogen. ChIP experiments were carried out with the Magnify ChIP assays (Life Technologies) according to the manufacturer's protocol. Briefly, 2 million cells were cross-linked with 1% formaldehyde, washed with cold PBS, and lysed in buffer containing protease inhibitors (Roche). Cell lysates were sonicated to shear DNA and sedimented, and diluted supernatants were immunoprecipitated with the indicated antibodies. 10% of the diluted supernatants were kept as "input" (input represents PCR amplification of the total sample). Real-time PCR primer sequences are given in Supplemental Table 1. The amount of immunoprecipitated DNA was subtracted from the amount of amplified DNA, which was bound by the nonspecific normal IgG and subsequently calculated as relative to the respective input DNA.

tants were collected and an identical amount of protein from each lysate (5 μg/well) was separated on NuPAGE 4%–12% Bis-Tris Gel (Life Technologies). Proteins were transferred to a nitrocellulose or PVDF membrane, which was subsequently blocked for 1 hour using 2% BSA in PBS and incubated at room temperature with anti-CaMK4 (Cell Signaling Technology), anti-AKT (Cell Signaling Technology), anti-phospho (Ser473)-AKT (Cell Signaling Technology), anti-S6K (Cell Signaling Technology), anti-phospho (Thr389)-S6K (Cell Signaling Technology), and anti-actin (Sigma-Aldrich). The membrane was washed with TBS-T and incubated with a 1:3,000 dilution of goat anti-rabbit IgG or donkey anti-goat IgG coupled with HRP (Jackson Immunoresearch). The ECL system (Amersham) was used for detection. Bands on blots corresponding to proteins of interest were analyzed by ImageJ software.

Immunoprecipitation. Immunoprecipitation was performed with the Dynabeads Protein G Immunoprecipitation Kit (Life Technologies) according to the manufacturer's protocol. Briefly, cell lysates were prepared as described above, and proteins were immunoprecipitated by incubation of lysates with 3 μg CaMK4 antibody or control rabbit IgG overnight at 4°C and pull-down of antibody-protein precipitates with Dynabeads Protein G.

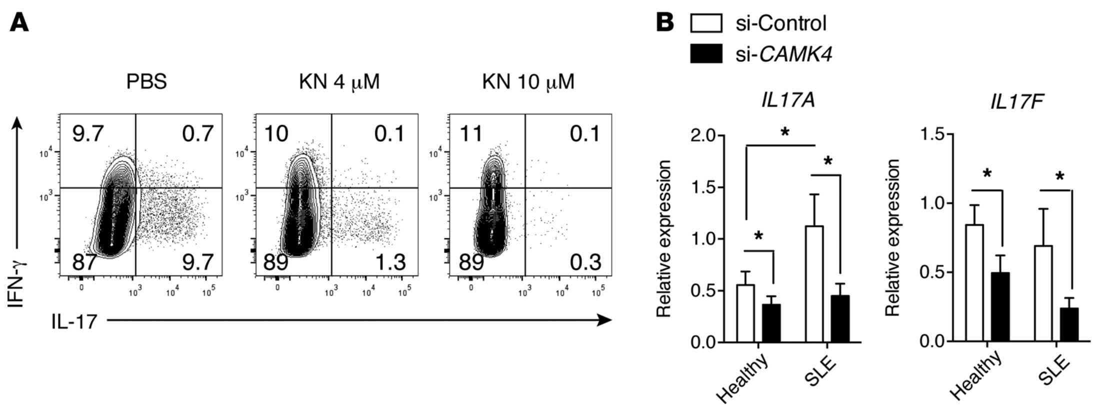

Figure 8
Silencing of CaMK4 decreases Th17 cells in patients with SLE. (**A**) T cells from healthy donors were stimulated in Th17 conditions in the absence or presence of KN-93 for 72 hours, and IFN-γ–producing CD4+ T cells or IL-17A–producing CD4+ T cells were determined by intracellular cytokine staining. A representative experiment from 1 of 4 donors is shown. (**B**) T cells from normal controls (n = 4) or patients with SLE (n = 6) were transfected with either control siRNA or *CAMK4*-specific siRNA. 24 hours after transfection, cells were differentiated for 72 hours under Th17 conditions and analyzed by quantitative real-time PCR of *IL17A* or *IL17F* mRNA (*P < 0.05; mean ± SEM).

Beads were washed extensively, and proteins were eluted with the elution buffer. The presence of immunocomplexed proteins was determined by Western blot analysis with AKT antibody.

Human SLE T cells. All patients with SLE included in our studies were diagnosed according to the American College of Rheumatology classification criteria (64). Patients with SLE were recruited from the Division of Rheumatology at Beth Israel Deaconess Medical Center and provided written informed consent under protocol 2006-P-0298, as approved by the Institutional Review Board. Age-, sex-, and ethnicity-matched healthy individuals were chosen as controls. Peripheral venous blood was collected in heparin-lithium tubes and total human T cells were purified as described previously (19–21).

Obtained T cells from these groups were treated with KN-93 or transfected with *CAMK4*-specific or control siRNA as described previously (20, 21). After 24 hours, cells were stimulated with plate-bound goat anti-mouse antibodies (Chemicon Millipore), soluble anti-CD3 (5 μg/ml, clone OKT3; BioXcell), anti-CD28 (2.5 μg/ml, clone 28.2; BioLegend), IL-6 (50 ng/ml, R&D Systems), and TGF-β1 (5 ng/ml, R&D Systems) and cultured for 96 hours.

Luciferase assays in Jurkat T cells. Reporter constructs spanning the proximal 195 bp of the human IL-17A promoter and site-directed mutagenesis at CRE site (–111/–104) and ROR element binding site (–140/–135) within reporter construct IL17Ap(–195)-luc have been described previously (35). Two million Jurkat T cells were transfected with 500 ng per

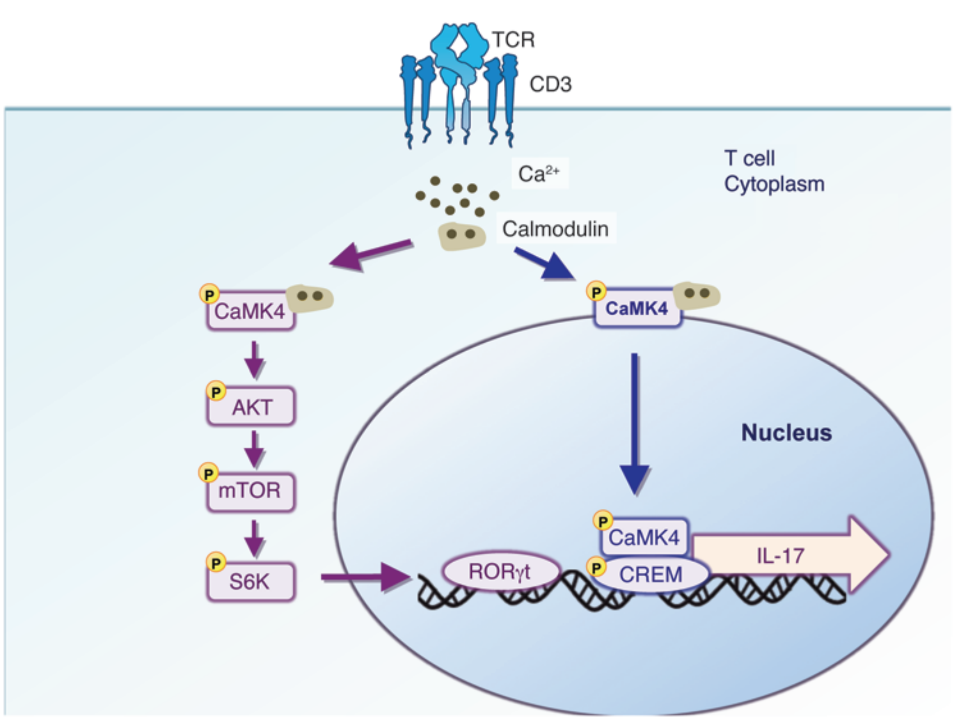

Figure 9
Model depicting the molecular mechanisms whereby CaMK4 controls the expression of IL-17. Engagement of the TCR causes an increase in intracellular calcium that leads to the activation of CaMK4. Active CaMK4 translocates to the nucleus, in which it phosphorylates CREM-α, which can bind to *Il17* promoter. On the other hand, active CaMK4 also phosphorylates AKT, resulting in the activation of the AKT/mTOR/S6K pathway. S6K interacts with RORγ and enhances its nuclear translocation, leading to transcriptional control of IL-17.

10^6 cells of plasmid DNA using the Amaxa Human T cell Nucleofector Kit (Lonza) and an Amaxa Nucleofector II device (program U014; Lonza). Each reporter experiment included 10 ng renilla luciferase construct as an internal control. 12 hours after transfection, cells were stimulated with anti-CD3 and anti-CD28 antibodies in the absence or presence of KN-93 for 6 hours and collected and lysed, and luciferase activity was quantified using the Promega Dual Luciferase Assay System (Promega) following the manufacturer's instructions.

Infection with lentivirus. Jurkat T cells were infected with CaMK4-inducible lentivirus particles (LVP133; GenTarget) or negative control lentiviral particles (RFP-Bsd; GenTarget). At 3 days after transduction, cells were stimulated with anti-CD3 and anti-CD28 antibodies, and phosphorylation of AKT and S6K was examined by flow cytometry.

Statistics. Student's 2-tailed *t* tests and Mann Whitney tests were used. Statistical analyses were performed in GraphPad Prism 6.0b software. $P < 0.05$ was considered significant.

Acknowledgments

This work was supported by NIH grant R01AR064350 (to G.C. Tsokos). We wish to thank Maria Tsokos for evaluating the spinal cord histology.

Received for publication October 4, 2013, and accepted in revised form January 23, 2014.

Address correspondence to: George C. Tsokos, Beth Israel Deaconess Medical Center, Harvard Medical School, 330 Brookline Ave., CLS-937, Boston, Massachusetts 02215, USA. Phone: 617.735.4160; Fax: 617.735.4170; E-mail: gtsokos@bidmc.harvard.edu. Or to: Jose C. Crispin, Beth Israel Deaconess Medical Center, Harvard Medical School, 330 Brookline Ave., Dana-517C, Boston, Massachusetts 02215, USA. Phone: 617.667.2786; Fax: 617.667.2785; E-mail: jcrispin@bidmc.harvard.edu.

1. Harrington LE, et al. Interleukin 17-producing CD4+ effector T cells develop via a lineage distinct from the T helper type 1 and 2 lineages. *Nat Immunol*. 2005;6(11):1123–1132.
2. Park H, et al. A distinct lineage of CD4 T cells regulates tissue inflammation by producing interleukin 17. *Nat Immunol*. 2005;6(11):1133–1141.
3. Korn T, Bettelli E, Oukka M, Kuchroo VK. IL-17 and Th17 cells. *Annu Rev Immunol*. 2009;27:485–517.
4. Di Cesare A, Di Meglio P, Nestle FO. The IL-23/Th17 axis in the immunopathogenesis of psoriasis. *J Invest Dermatol*. 2009;129(6):1339–1350.
5. Crispin JC, Tsokos GC. Interleukin-17-producing T cells in lupus. *Curr Opin Rheumatol*. 2010;22(5):499–503.
6. Montes M, et al. Oligoclonal myelin-reactive T-cell infiltrates derived from multiple sclerosis lesions are enriched in Th17 cells. *Clin Immunol*. 2009;130(2):133–144.
7. Tsokos GC. Systemic lupus erythematosus. *N Engl J Med*. 2011;365(22):2110–2121.
8. Nistala K, Moncrieffe H, Newton KR, Varsani H, Hunter P, Wedderburn LR. Interleukin-17-producing T cells are enriched in the joints of children with arthritis, but have a reciprocal relationship to regulatory T cell numbers. *Arthritis Rheum*. 2008;58(3):875–887.
9. Wing K, Sakaguchi S. Regulatory T cells exert checks and balances on self tolerance and autoimmunity. *Nat Immunol*. 2010;11(1):7–13.
10. Bettelli E, et al. Reciprocal developmental pathways for the generation of pathogenic effector TH17 and regulatory T cells. *Nature*. 2006;441(7090):235–238.
11. Frohman EM, Racke MK, Raine CS. Multiple sclerosis — the plaque and its pathogenesis. *N Engl J Med*. 2006;354(9):942–955.
12. Langrish CL, et al. IL-23 drives a pathogenic T cell population that induces autoimmune inflammation. *J Exp Med*. 2005;201(2):233–240.
13. Alunno A, et al. Balance between regulatory T and Th17 cells in systemic lupus erythematosus: the old and the new. *Clin Dev Immunol*. 2012;2012:823085.
14. Chen Y, et al. Foxp3(+) regulatory T cells promote T helper 17 cell development in vivo through regulation of interleukin-2. *Immunity*. 2011;34(3):409–421.
15. Laurence A, et al. Interleukin-2 signaling via STAT5 constrains T helper 17 cell generation. *Immunity*. 2007;26(3):371–381.
16. Liao W, Lin JX, Wang L, Li P, Leonard WJ. Modulation of cytokine receptors by IL-2 broadly regulates differentiation into helper T cell lineages. *Nat Immunol*. 2011;12(6):551–559.
17. Lieberman LA, Tsokos GC. The IL-2 defect in systemic lupus erythematosus disease has an expansive effect on host immunity. *J Biomed Biotechnol*. 2010;2010:740619.
18. Racioppi L, Means AR. Calcium/calmodulin-dependent kinase IV in immune and inflammatory responses: novel routes for an ancient traveller. *Trends Immunol*. 2008;29(12):600–607.
19. Juang YT, et al. Systemic lupus erythematosus serum IgG increases CREM binding to the IL-2 promoter and suppresses IL-2 production through CaMKIV. *J Clin Invest*. 2005;115(4):996–1005.
20. Koga T, Ichinose K, Mizui M, Crispin JC, Tsokos GC. Calcium/calmodulin-dependent protein kinase IV suppresses IL-2 production and regulatory T cell activity in lupus. *J Immunol*. 2012;189(7):3490–3496.
21. Ichinose K, Juang YT, Crispin JC, Kis-Toth K, Tsokos GC. Suppression of autoimmunity and organ pathology in lupus-prone mice upon inhibition of calcium/calmodulin-dependent protein kinase type IV. *Arthritis Rheum*. 2011;63(2):523–529.
22. Ichinose K, et al. Cutting edge: calcium/calmodulin-dependent protein kinase type IV is essential for mesangial cell proliferation and lupus nephritis. *J Immunol*. 2011;187(11):5500–5504.
23. Chen W, et al. Conversion of peripheral $CD4^+CD25^-$ naive T cells to $CD4^+CD25^+$ regulatory T cells by TGF-β induction of transcription factor Foxp3. *J Exp Med*. 2003;198(12):1875–1886.
24. Sutton C, Brereton C, Keogh B, Mills KH, Lavelle EC. A crucial role for interleukin (IL)-1 in the induction of IL-17-producing T cells that mediate autoimmune encephalomyelitis. *J Exp Med*. 2006;203(7):1685–1691.
25. Wayman GA, Tokumitsu H, Davare MA, Soderling TR. Analysis of CaM-kinase signaling in cells. *Cell Calcium*. 2011;50(1):1–8.
26. Zhang Z, Kyttaris VC, Tsokos GC. The role of IL-23/IL-17 axis in lupus nephritis. *J Immunol*. 2009;183(5):3160–3169.
27. Redondo RL, Okuno H, Spooner PA, Frenguelli BG, Bito H, Morris RG. Synaptic tagging and capture: differential role of distinct calcium/calmodulin kinases in protein synthesis-dependent long-term potentiation. *J Neurosci*. 2010;30(14):4981–4989.
28. Wekerle H. Lessons from multiple sclerosis: models, concepts, observations. *Ann Rheum Dis*. 2008;67(suppl 3):iii56–iii60.
29. Mendel I, Kerlero de Rosbo N, Ben-Nun A. A myelin oligodendrocyte glycoprotein peptide induces typical chronic experimental autoimmune encephalomyelitis in H-2b mice: fine specificity and T cell receptor V beta expression of encephalitogenic T cells. *Eur J Immunol*. 1995;25(7):1951–1959.
30. Pisitkun P, et al. Interleukin-17 cytokines are critical in development of fatal lupus glomerulonephritis. *Immunity*. 2012;37(6):1104–1115.
31. Kyttaris VC, Zhang Z, Kuchroo VK, Oukka M, Tsokos GC. Cutting edge: IL-23 receptor deficiency prevents the development of lupus nephritis in C57BL/6-lpr/lpr mice. *J Immunol*. 2010;184(9):4605–4609.
32. Ivanov II, et al. The orphan nuclear receptor RORgammat directs the differentiation program of proinflammatory $IL-17^+$ T helper cells. *Cell*. 2006;126(6):1121–1133.
33. Fatemi M, et al. Footprinting of mammalian promoters: use of a CpG DNA methyltransferase revealing nucleosome positions at a single molecule level. *Nucleic Acids Res*. 2005;33(20):e176.
34. Hedrich CM, Rauen T, Tsokos GC. cAMP-responsive element modulator (CREM)α protein signaling mediates epigenetic remodeling of the human interleukin-2 gene: implications in systemic lupus erythematosus. *J Biol Chem*. 2011;286(50):43429–43436.
35. Rauen T, Hedrich CM, Juang YT, Tenbrock K, Tsokos GC. cAMP-responsive element modulator (CREM)α protein induces interleukin 17A expression and mediates epigenetic alterations at the interleukin-17A gene locus in patients with systemic lupus erythematosus. *J Biol Chem*. 2011;286(50):43437–43446.
36. Liu XK, Lin X, Gaffen SL. Crucial role for nuclear factor of activated T cells in T cell receptor-mediated regulation of human interleukin-17. *J Biol Chem*. 2004;279(50):52762–52771.
37. Kurebayashi Y, et al. PI3K-Akt-mTORC1-S6K1/2 axis controls Th17 differentiation by regulating Gfi1 expression and nuclear translocation of RORγ. *Cell Rep*. 2012;1(4):360–373.
38. Delgoffe GM, et al. The kinase mTOR regulates the differentiation of helper T cells through the selective activation of signaling by mTORC1 and mTORC2. *Nat Immunol*. 2011;12(4):295–303.
39. Kim JS, et al. Natural and inducible TH17 cells are regulated differently by Akt and mTOR pathways. *Nat Immunol*. 2013;14(6):611–618.
40. Yano S, Tokumitsu H, Soderling TR. Calcium promotes cell survival through CaM-K kinase activation of the protein-kinase-B pathway. *Nature*. 1998;396(6711):584–587.
41. Rokhlin OW, et al. Calcium/calmodulin-dependent kinase II plays an important role in prostate cancer cell survival. *Cancer Biol Ther*. 2007;6(5):732–742.
42. Doreau A, et al. Interleukin 17 acts in synergy with B cell-activating factor to influence B cell biology and the pathophysiology of systemic lupus erythematosus. *Nat Immunol*. 2009;10(7):778–785.
43. Wong CK, Lit LC, Tam LS, Li EK, Wong PT, Lam CW. Hyperproduction of IL-23 and IL-17 in patients with systemic lupus erythematosus: implications for Th17-mediated inflammation in auto-immunity. *Clin Immunol*. 2008;127(3):385–393.
44. Nalbandian A, Crispin JC, Tsokos GC. Interleukin-17 and systemic lupus erythematosus: current

concepts. *Clin Exp Immunol*. 2009;157(2):209–215.
45. Hsu HC, et al. Interleukin 17-producing T helper cells and interleukin 17 orchestrate autoreactive germinal center development in autoimmune BXD2 mice. *Nat Immunol*. 2008;9(2):166–175.
46. Kozyrev SV, et al. Functional variants in the B-cell gene BANK1 are associated with systemic lupus erythematosus. *Nat Genet*. 2008;40(2):211–216.
47. Crispin JC, et al. Expanded double negative T cells in patients with systemic lupus erythematosus produce IL-17 and infiltrate the kidneys. *J Immunol*. 2008;181(12):8761–8766.
48. Shevach EM. Mechanisms of foxp3+ T regulatory cell-mediated suppression. *Immunity*. 2009; 30(5):636–645.
49. Valencia X, Yarboro C, Illei G, Lipsky PE. Deficient $CD4^+CD25^{high}$ T regulatory cell function in patients with active systemic lupus erythematosus. *J Immunol*. 2007;178(4):2579–2588.
50. Bonelli M, Smolen JS, Scheinecker C. Treg and lupus. *Ann Rheum Dis*. 2010;69(suppl 1):i65–i66.
51. Patel DR, Richardson BC. Dissecting complex epigenetic alterations in human lupus. *Arthritis Res Ther*. 2013;15(1):201.
52. Strickland FM, et al. Diet influences expression of autoimmune-associated genes and disease severity by epigenetic mechanisms in a transgenic mouse model of lupus. *Arthritis Rheum*. 2013;65(7):1872–1881.
53. Hedrich CM, et al. cAMP response element modulator alpha controls IL2 and IL17A expression during CD4 lineage commitment and subset distribution in lupus. *Proc Natl Acad Sci U S A*. 2012;109(41):16606–16611.
54. Hedrich CM, et al. cAMP responsive element modulator (CREM)alpha mediates chromatin remodeling of CD8 during the generation of $CD3^+CD4^-CD8^-$ T cells. *J Biol Chem*. 2014;289(4):2361–2370.
55. Tenbrock K, Juang YT, Gourley MF, Nambiar MP, Tsokos GC. Antisense cyclic adenosine 5′-monophosphate response element modulator up-regulates IL-2 in T cells from patients with systemic lupus erythematosus. *J Immunol*. 2002;169(8):4147–4152.
56. Laplante M, Sabatini DM. mTOR signaling in growth control and disease. *Cell*. 2012;149(2):274–293.
57. Reddy PS, et al. Mapping similarities in mTOR pathway perturbations in mouse lupus nephritis models and human lupus nephritis. *Arthritis Res Ther*. 2008;10(6):R127.
58. Warner LM, Adams LM, Sehgal SN. Rapamycin prolongs survival and arrests pathophysiologic changes in murine systemic lupus erythematosus. *Arthritis Rheum*. 1994;37(2):289–297.
59. Fernandez D, Bonilla E, Mirza N, Niland B, Perl A. Rapamycin reduces disease activity and normalizes T cell activation-induced calcium fluxing in patients with systemic lupus erythematosus. *Arthritis Rheum*. 2006;54(9):2983–2988.
60. Dittrich E, Schmaldienst S, Soleiman A, Horl WH, Pohanka E. Rapamycin-associated post-transplantation glomerulonephritis and its remission after reintroduction of calcineurin-inhibitor therapy. *Transpl Int*. 2004;17(4):215–220.
61. Thaunat O, et al. Anemia after late introduction of sirolimus may correlate with biochemical evidence of a chronic inflammatory state. *Transplantation*. 2005;80(9):1212–1219.
62. Weichhart T, Saemann MD. The multiple facets of mTOR in immunity. *Trends Immunol*. 2009; 30(5):218–226.
63. Hedrich CM, Tsokos GC. Epigenetic mechanisms in systemic lupus erythematosus and other autoimmune diseases. *Trends Mol Med*. 2011;17(12):714–724.
64. Tan EM, et al. The 1982 revised criteria for the classification of systemic lupus erythematosus. *Arthritis Rheum*. 1982;25(11):1271–1277.